

# Verification of Electromagnetic Fully-kinetic Symplectic Particle-in-cell Method in Microinstabilities Simulation of Toroidal Plasmas

Jianyuan Xiao<sup>1</sup> and Jian liu<sup>2,3,\*</sup>

<sup>1</sup>*Department of Plasma Physics and Fusion Engineering,  
University of Science and Technology of China, Hefei, 230026, China*

<sup>2</sup>*Weihai Institute for Interdisciplinary Research,  
Shandong University, Weihai 264209, China*

<sup>3</sup>*SDU-ANU Joint Science College, Shandong University, Weihai 264209, China*

## Abstract

We present a symplectic electromagnetic fully-kinetic particle-in-cell simulation of microinstabilities in plasma, using parameters from the Cyclone Base Case [Dimits, et al., Physics of Plasmas 7, 969 (2000)]. The results show that the growth rates of unstable modes, including ion temperature gradient (ITG), trapped electron mode (TEM), and kinetic ballooning mode (KBM), are consistent with those obtained from previous gyrokinetic models. Additionally, the  $\beta$ -stabilization of the ITG is reproduced. The analysis also reveals that the impact of the ion-electron mass ratio and the numerical speed of light on the growth rate of the most unstable modes is minimal. This suggests that the fully kinetic method offers a potential for reduced computational cost when investigating the physics of drift wave instabilities at relevant space-time scales.

PACS numbers: 52.65.Rr, 52.35.Qz, 52.35.Ra, 52.25.Dg

---

\* Corresponding Author: [liu\\_jian@sdu.edu.cn](mailto:liu_jian@sdu.edu.cn)

## I. INTRODUCTION

It is widely believed that microinstability-driven turbulence is a key factor in the anomalous transport [1] of plasmas, which significantly impacts the performance of magnetic confinement fusion devices. These instabilities arise primarily from steep temperature and density gradients within the plasma. Typically, a gyrokinetic [2–4] approach is used to model this kind of turbulence. Previous electromagnetic gyrokinetic methods [5–7] have identified three types of microinstabilities at the ion motion scale, i.e., Ion Temperature Gradient (ITG), Trapped Electron Mode (TEM), and Kinetic Ballooning Modes (KBM) instabilities. The dominant unstable mode varies with plasma parameters, and simulations indicate that as plasma beta increases, these microinstabilities initially stabilize before becoming unstable once beta surpasses the so-called ballooning limit [8].

Conventional gyrokinetic models simplify the evolution of both particle and electromagnetic fields compared to fully-kinetic charged particle-electromagnetic models, raising concerns about the impact of these simplifications on results. With the advent of 100 petaflop and exaflop supercomputers, it is now feasible to directly simulate microinstabilities in whole-volume magnetic fusion plasmas using fully-kinetic particle-in-cell (PIC) methods. This allows for verification of previous gyrokinetic models and the potential discovery of new physics that may not be captured by those models. However, traditional full-kinetic PIC methods face significant challenges when simulating charged particle-electromagnetic fields systems. First, the grid size must resolve the Debye radius ( $\lambda_D$ ), such as in the Boris-Yee scheme, to avoid self-heating from finite-sized grid instabilities [9–11], which is problematic as the Debye radius in magnetic confinement fusion plasmas is typically much smaller than the global plasma size. For instance, with typical fusion plasma temperatures of  $T_e \sim 10\text{keV}$  and density of  $1 \times 10^{20}\text{m}^{-3}$ , the Debye radius is less than 0.1mm, necessitating over 10,000 grids in each direction to resolve it in a typical plasma size about 1m, leading to computational demands that are currently unmanageable. Additionally, the time-step in conventional explicit PIC schemes is limited by the Courant-Friedrichs-Lowy (CFL) condition and plasma frequency ( $\omega_{pe}$ ), requiring over a million time-steps to resolve one period of unstable modes. This long-term simulation can accumulate significant numerical errors, compromising result reliability.

To address these issues, we employed a newly developed explicit 2nd-order charge-

conservative symplectic structure-preserving electromagnetic fully-kinetic (FK) PIC scheme for cylindrical geometry [12, 13] to simulate microinstabilities using the established Cyclone Base Case (CBC) [14] parameters. This method eliminates the self-heating problem, and its superior long-term conservative properties ensure result accuracy. We identify frequency and growth rate of unstable modes and our findings include: 1) The growth rates of ITG and TEM from the FK method are slightly higher than predictions from gyrokinetic models, while the KBM growth rate is comparable. 2) The mode frequencies for ITG and TEM align closely with gyrokinetic predictions, whereas the KBM frequency is lower than expected. 3) The growth rate of the most unstable mode initially decreases with increasing plasma beta for ITG and TEM, while it significantly increases for KBM, consistent with previous electromagnetic gyrokinetic simulations.

This paper is organized as follows. Section 2 provides a brief introduction to the electromagnetic fully kinetic physical model and the symplectic structure-preserving method. Section 3 details the construction of Tokamak equilibrium, including Cyclone Base Case parameters and simulation results. Finally, Section 4 concludes the paper.

## II. SYMPLECTIC ELECTROMAGNETIC FULLY-KINETIC PARTICLE-IN-CELL SCHEME EMPLOYED IN SYMPIC

First, we briefly introduce the symplectic electromagnetic fully-kinetic PIC scheme in the cylindrical coordinate developed previously [12] which is implemented in SymPIC code and it can run efficiently on modern heterogeneous supercomputers with up to over 40 million cores [13]. Previously, we have applied it to simulate Tokamak edge plasmas and obtained comparable results with fluid simulations and experiments [15]. In this work, we focus on verifying of simulations of microinstabilities in core plasmas using this approach.

This work focuses on the physical model of charged particles coupled with electromagnetic fields, of which the evolution equations are

$$\ddot{\mathbf{x}}_{s,p} = \frac{q_s}{m_s} (\mathbf{E}(\mathbf{x}_{s,p}) + \dot{\mathbf{x}}_{s,p} \times \mathbf{B}(\mathbf{x}_{s,p})) , \quad (1)$$

$$\dot{\mathbf{E}} = \nabla \times \mathbf{B} - \sum_{s,p} q_s \dot{\mathbf{x}}_{s,p} \delta(\mathbf{x} - \mathbf{x}_{s,p}) , \quad (2)$$

$$\dot{\mathbf{B}} = -\nabla \times \mathbf{E} , \quad (3)$$

where  $\mathbf{x}_{s,p}, m_s, q_s$  indicates the location, mass, charge of the  $p$ -th particle of the  $s$ -species,

$\mathbf{E}$  and  $\mathbf{B}$  are electromagnetic fields. For simplicity, we normalize both permittivity  $\epsilon_0$  and permeability  $\mu_0$  in the vacuum to 1. To build symplectic structure preserving PIC method in the cylindrical geometry, we start from the action integral of the charged particle coupled with electromagnetic fields system, which reads

$$\begin{aligned}\mathcal{A}[\mathbf{x}_{sp}, \dot{\mathbf{x}}_{sp}, \mathbf{A}, \phi] = & \int dt \sum_{s,p} (L_{sp}(m_s, \mathbf{v}_{sp}) + q_s (\mathbf{v}_{sp} \cdot \mathbf{A}(\mathbf{x}_{sp}, t) - \phi(\mathbf{x}_{sp}, t))) \\ & + \int dV dt \frac{1}{2} \left( (-\dot{\mathbf{A}}(\mathbf{x}, t) - \nabla \phi(\mathbf{x}, t))^2 - (\nabla \times \mathbf{A}(\mathbf{x}, t))^2 \right),\end{aligned}\quad (4)$$

where  $\mathbf{x} = [x_1, x_2, x_3]$  and  $dV = |h_1(\mathbf{x}) h_2(\mathbf{x}) h_3(\mathbf{x})| dx_1 dx_2 dx_3$ . In cylindrical coordinate, we choose line elements as

$$h_1(x_1, x_2, x_3) = 1, \quad (5)$$

$$h_2(x_1, x_2, x_3) = (x_1/X_0 + 1) \Delta x_2 / \Delta x_1, \quad (6)$$

$$h_3(x_1, x_2, x_3) = \Delta x_3 / \Delta x_1. \quad (7)$$

Here  $\Delta x_1, \Delta x_2$  and  $\Delta x_3$  are reference grid size for each direction,  $X_0$  is the location of inner boundary of the simulation domain. Hence the velocity of each particle is

$$\mathbf{v}_{sp} = [\dot{x}_{1,sp} h_1, \dot{x}_{2,sp} h_2, \dot{x}_{3,sp} h_3], \quad (8)$$

where

$$[x_{1,sp}, x_{2,sp}, x_{3,sp}] = \mathbf{x}_{sp} \quad (9)$$

is the coordinate of each particle in the cylindrical geometry. Finally the Lagrangian for each particle is

$$L_{sp}(m_s, \mathbf{v}_{sp}) = \frac{1}{2} m_s \mathbf{v}_{sp}^2, \quad (10)$$

and the electromagnetic fields are defined as

$$\mathbf{E} = -\dot{\mathbf{A}} - \nabla \phi, \quad (11)$$

$$\mathbf{B} = \nabla \times \mathbf{A}. \quad (12)$$

The evolution equations Eqs. (1)-(3) can be derived from variation, i.e.,

$$\frac{\delta \mathcal{A}}{\delta \mathbf{x}_{sp}} = 0, \quad (13)$$

$$\frac{\delta \mathcal{A}}{\delta \mathbf{A}} = 0, \quad (14)$$

$$\frac{\delta \mathcal{A}}{\delta \phi} = 0, \quad (15)$$

and the key to build symplectic algorithm is to find the discrete action integral. According to our previous work [13], the action integral can be discretized using Discrete Exterior Calculus (DEC), Whitney interpolating form and zigzag integral path of particles to guarantee the discrete gauge invariance property. In such discretization, local charge conservation property is automatically satisfied and hence we can directly use electromagnetic fields rather than potentials to build the algorithm. Then the final explicit iteration scheme can be obtained by using discrete variational method or Hamiltonian splitting technique. Detail of the 2nd-order charge-conservative symplectic PIC scheme for the cylindrical coordinate can be found in the Appendix B of Ref. [13]. In the present work, the Whitney interpolating 0-form in slab geometry is chosen as

$$W_{\sigma_0 I}(\mathbf{x}) = W_1(x_1) W_1(x_2) W_1(x_3) , \quad (16)$$

where

$$W_1(x) = \begin{cases} 0, & x < -2 \\ \frac{(x+2)^2}{4}, & -2 \leq x < -1 \\ \frac{2-x^2}{4}, & -1 \leq x < 1 \\ \frac{(x-2)^2}{4}, & 1 \leq x < 2 \\ 0, & x \geq 2 . \end{cases} \quad (17)$$

The present method offers several advantages over previous gyrokinetic methods. 1) It treats charged particles as fully kinetic, avoiding the gyro-average or guiding center approximation of charged particles. 2) The model of fields is complete electromagnetic, incorporating electromagnetic waves, unlike previous gyrokinetic methods that ignore the displacement current term  $\partial\mathbf{E}/\partial t$  in the Maxwell equation. 3) The model includes both the parallel and perpendicular components of the magnetic potential, accounting for the effects of both shear Alfvén and compressible magnetosonic waves, which are often simplified in earlier electromagnetic gyrokinetic models. Due to the computational cost constraints, using a reduced speed of light in vacuum and a reduced ion-electron mass ratio is preferred for real simulations. However, the impact of these reductions on the results remains uncertain and will be explored in this study.

### III. SIMULATION OF INSTABILITIES IN CORE PLASMAS

The Cyclone Base Case (CBC) parameters, typically used to benchmark gyrokinetic algorithms, [14, 16, 17] characterize a local Tokamak plasma. They can be listed as follows. The minor radius  $r = 0.5a$ , where  $a$  is the minor radius of the last closed flux surface. The shape of poloidal cross section is circular, with  $n_i = n_e$ ,  $T_i = T_e$ , where  $n_i$ ,  $n_e$ ,  $T_i$ ,  $T_e$  are the ion density, electron density, ion temperature and electron temperature, respectively. The parameter values in dimensionless form are  $\eta_i = L_n/L_T = 3.114$ , where  $L_n$  and  $L_T$  are the density and temperature gradient scale lengths, respectively, safety factor which is chosen as  $q = rB_t/R_0B_p = 1.4$ , where  $R_0$  is the major radius and  $B_t$  and  $B_p$  are the toroidal and poloidal magnetic field components,  $\hat{s} = (r/q)dq/dr = 0.8$ ,  $R_0/L_T = 6.92$ , and  $a/R_0 = 0.36$ . We build initial conditions for kinetic particles and magnetic field from the 2D solution that satisfying the above local conditions generated by a Free boundary Grad-Shafranov solver (FreeGS) [18], then perform a 2D-3V (i.e.,  $N_\theta = 1$ ) simulation using SymPIC to generate a relatively stable kinetic equilibrium as the final initial condition for 3D-3V simulation. The gyro-radius of thermal speed for ions at  $r$  is set to  $\rho^* = m_i\sqrt{T_i/m_i}/(q_iB_0) \sim a/147$ , and we tested various plasma betas of electrons, i.e.,  $\beta_e = 0.17\%, 0.58\%, 0.87\%, 1.16\%$  and  $1.45\%$ . According to previous results based on gyrokinetic simulations, [5–7] growth rate of microinstabilities such as ion temperature gradient (ITG) and trapped electron modes (TEM) will become small with the increment of plasma beta. Simulation domain is a 1/3 ring, i.e.,  $R_{\text{left}} \leq R < R_{\text{left}} + 1.033R_0$ ,  $0 \leq \theta < 2\pi/3$ ,  $0 < z < 1.381R_0$ ,  $R_0 = 0.958\text{m}$ ,  $R_{\text{left}} = 0.437R_0$ , where

$$R = x_1\Delta x_1 + R_{\text{left}}, \quad (18)$$

$$\theta = x_2\Delta x_2/R_{\text{left}}, \quad (19)$$

$$z = x_3\Delta x_3, \quad (20)$$

$$\Delta x_1 = 1.033R_0/N_R, \quad (21)$$

$$\Delta x_2 = (2\pi/3)R_{\text{left}}/N_\theta, \quad (22)$$

$$\Delta x_3 = 1.33\Delta x_1, \quad (23)$$

and number of grids in  $R, \theta, z$  directions  $N_R, N_z$  and  $N_\theta$  are set to  $N_R = N_z = 256$ ,  $N_\theta = 64$ . Timestep is set to  $2.02 \times 10^{-3}R_0/c_N$  where  $c_N$  is the numerical speed of light in vacuum in the simulations. To reduce the computational complexity,  $c_N$  is set to  $0.225c$  where

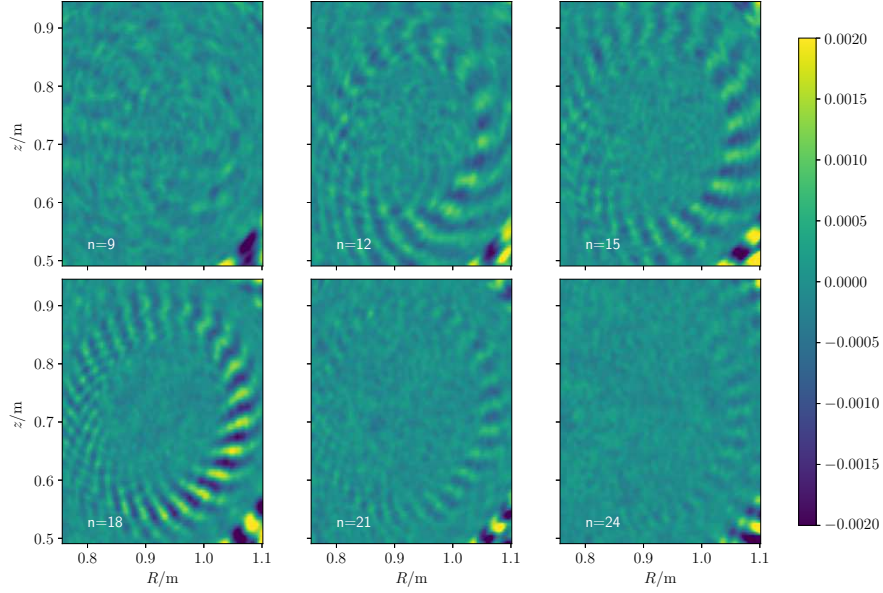


Figure 1: Unstable mode structures of density perturbation for different toroidal mode number  $n$  in CBC-like plasma with ITG parameters, here  $tv_{ti}/R_0 \sim 10.35$  and  $\beta_e = 0.17\%$ .

$c$  is real speed of light in vacuum, mass of electron is set to  $m_e = m_i/100$ , ions are all deuterium. Thermal speeds and densities of electrons and ions at the magnetic axis are set to  $v_{te} = 10v_{ti} = 0.0447c_N$  and  $n_e = n_i = 2.65 \times 10^{21}\beta_e m^{-3}$ , respectively. Total number of time-steps is  $N_t = 2 \times 10^6$ , which is about  $N_t \Delta t \sim 4.7 \times 10^3 \omega_{ci}^{-1} \sim 18R_0/v_{ti}$ . The maximum number of sampling particle in one grid cell for each species ranges from 1000 – 4000 dependending on different parameters. One above 3D-3V simulation requires approximately  $1 \times 10^5$  to  $4 \times 10^5$  core hours CPU time on the new Sunway supercomputer.

Structures of unstable modes for  $\beta_e = 0.17\%$ ,  $1.16\%$  and  $1.45\%$  are shown in Figs. 1-3. For  $\beta_e = 1.45\%$  case, due to the large Shafranov shift, we modify  $R_{left}$  as  $R_{left} = 0.509R_0$ , corresponding new major radius is  $R_{0,KBM} = 1.06R_0$ . mode number of the most unstable mode is  $n = 18$ , so the corresponding  $k_\theta = nq/r$  complies  $k_\theta \rho_i = 0.34$  which is consistent with previous electrostatic gyrokinetic (ESGK) simulations [16]. Here in our simulation all toroidal modes are nonlinearly coupled together, so the growth rate of unstable toroidal modes may different from that obtained by conventional methods in which only one toroidal mode is included. To see how the ion-electron mass ratio and numerical speed of light effect the results, we also perform 3 extra cases with the changing of parameters listed in Tab. I, and other parameters remains the same as the  $\beta_e = 0.18\%$  case. We plotted growth rates

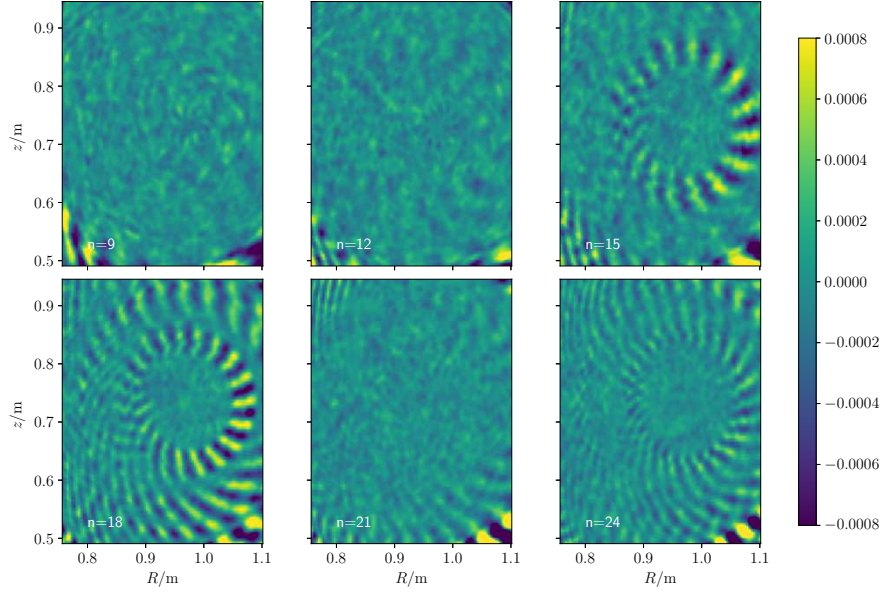


Figure 2: Unstable mode structures of density perturbation for different toroidal mode number  $n$  in CBC-like plasma with TEM parameters, here  $tv_{ti}/R_0 \sim 9.35$  and  $\beta_e = 1.16\%$ .

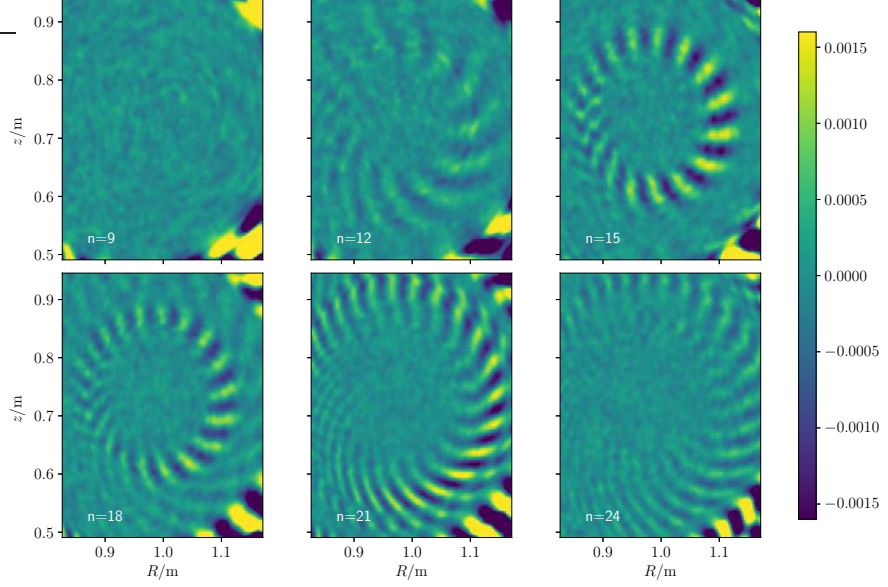


Figure 3: Unstable mode structures of density perturbation for different toroidal mode number  $n$  in CBC-like plasma with KBM parameters, here  $tv_{ti}/R_0 \sim 8.76$  and  $\beta_e = 1.45\%$ .

and frequencies of unstable modes obtained by SymPIC for these cases in Fig. 4, which shows that the growth rate of the most unstable mode is relatively independent from the

Extra Case No.	1	2	3
$m_i/m_e$	200	200	100
$c_N/c$	0.225	0.45	0.45

Table I: Parameters for testing the dependence of growth rates to the ion-electron mass ratio and the numerical speed of light.

ion-electron mass ratio and the numerical speed of light. The growth rate of unstable modes

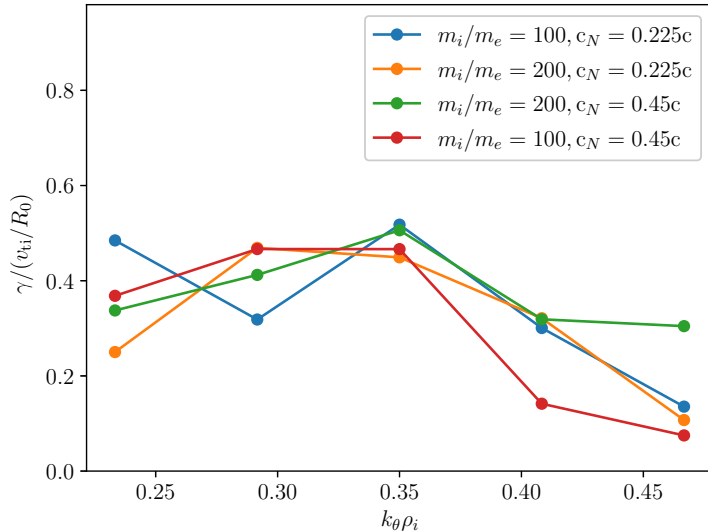


Figure 4: Dependence of the growth rate  $\gamma$  on the  $k_\theta$  obtained by SymPIC for  $m_i = 200m_e$  and  $m_i = 100m_e$

of plasmas with different  $\beta_e$  and  $k_\theta$  are presented in Fig. 5, we also show results obtained by previous ESGK ( $\beta_e = 0$ ) simulations for comparison. It can be seen that when  $\beta_e$  is low ( $\beta_e = 0.18\%$ ), growth rates obtained from electromagnetic fully-kinetic PIC scheme are in the same order of magnitude and roughly have the same trend with changes in  $k_\theta$ . When the pressure becomes high, the growth rate drops. To perform a more comprehensive comparison, frequency and growth rate of the most unstable mode obtained by the present fully-kinetic (FK) PIC method are plotted in Fig. 6. Electromagnetic gyrokinetic (GK) simulation results [7] are also plotted as reference. It is clear that the growth rate obtained by SymPIC and previous gyrokinetic methods are in the same order of magnitude and have

the same trend with changes in  $\beta_e$ .

The mode frequencies obtained by the FK method has large uncertainty (see the errorbars in Fig. 6a) due to the large noise of radial electric field in the PIC simulation. However they are also in the same order of magnitude compared with corresponding GK method, except for the KBM case. This may due to that converting the KBM frequency from the laboratory frame to the plasma frame requires no or more than subtraction of the  $\mathbf{E} \times \mathbf{B}$  velocity.

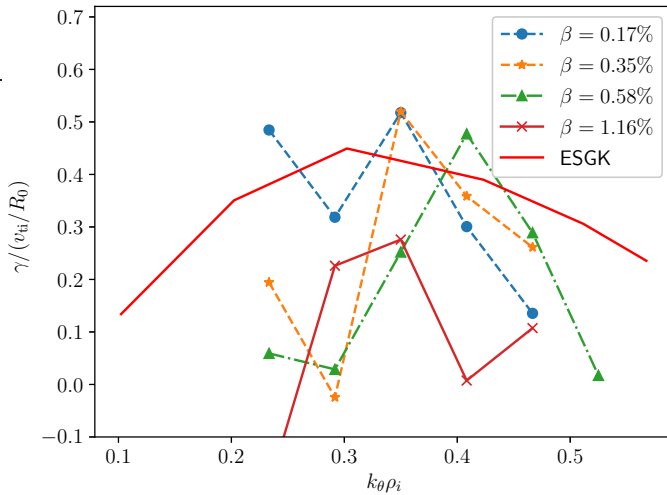


Figure 5: Dependence of the growth rate  $\gamma$  on the  $k_\theta$  obtained by SymPIC, ESGK ( $\beta_e = 0$ ) results [16] are also shown as reference.

#### IV. DISCUSSIONS AND CONCLUSIONS

In this study, we have presented a comprehensive investigation of microinstabilities in toroidal plasmas using a novel symplectic electromagnetic FK PIC simulation method. By employing the well-established CBC parameters, we have successfully verified the reliability of our fully-kinetic approach in capturing the growth rates and mode frequencies of key microinstabilities, including ITG, TEM, and KBM instabilities. The growth rate of the unstable mode obtained through the FK approach slightly differs from, yet remains within the same order of magnitude as, that derived from previous GK methods. These results thereby providing a robust benchmark for future studies.

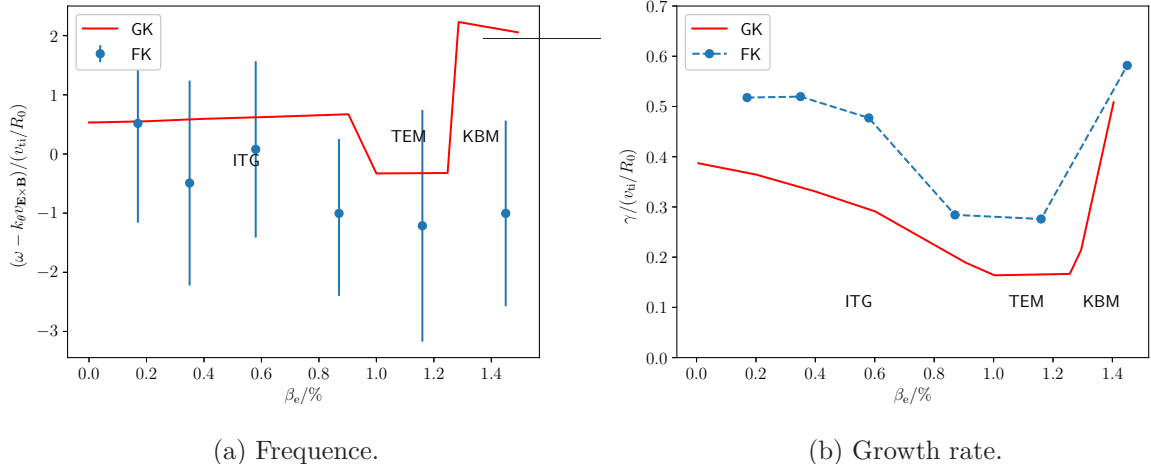


Figure 6: Dependence of frequency  $\omega - k_\theta v_{\mathbf{E} \times \mathbf{B}}$  and growth rate  $\gamma$  on the plasma  $\beta$  obtained by SymPIC. Electromagnetic GK results [7] are also shown as reference.

The FK PIC method employed in this work offers several significant advantages over traditional gyrokinetic approaches. It fully accounts for the kinetic nature of charged particles without relying on gyro-average or guiding center approximations. Additionally, it incorporates the complete electromagnetic field model, including the displacement current term often neglected in gyrokinetic simulations. This treatment allows for a more accurate representation of the underlying physics, especially in scenarios where electromagnetic effects and high-frequency phenomena play crucial roles.

Our simulations reveal that the growth rates of the most unstable modes are relatively insensitive to variations in the ion-electron mass ratio and the numerical speed of light. This finding suggests that the fully-kinetic method has the potential to significantly reduce computational costs when investigating drift wave instabilities at relevant space-time scales, making it a promising tool for large-scale simulations of magnetic fusion plasmas.

The results also highlight the  $\beta$ -stabilization effect on ITG instabilities and the contrasting behavior of KBM instabilities as plasma  $\beta$  increases. These observations align well with previous electromagnetic gyrokinetic simulations, further validating the accuracy and applicability of our fully-kinetic approach.

In conclusion, this study underscores the importance of employing fully-kinetic simulations to gain deeper insights into the complex dynamics of microinstabilities in toroidal

plasmas. The successful implementation of the SymPIC method on modern heterogeneous supercomputers demonstrates its potential for high-performance computing applications. Future work may focus on extending this approach to more complex plasma configurations and exploring additional physics phenomena that could be uncovered through fully-kinetic simulations. Overall, the findings presented here pave the way for more accurate and efficient modeling of plasma microinstabilities, ultimately contributing to the advancement of magnetic fusion research.

## ACKNOWLEDGMENTS

This work was supported by the Strategic Priority Research Program of Chinese Academy of Sciences (Grant No. XDB0500302), the National MC Energy R&D Program (2024YFE03020004, 2018YFE0304100), and the National Natural Science Foundation of China (NSFC-11905220 and 11805273). J. Xiao would like to thank Prof. Jinlin Xie and Prof. Weixing Ding at University of Science and Technology of China for valuable discussions on physics of drift wave instabilities. Simulations are performed in the New Sunway supercomputer, Tianhe-3A prototype machine, Hanhai20 of the USTC.

---

- [1] W. Horton, *Reviews of Modern Physics* **71**, 735 (1999).
- [2] W. Lee, *The Physics of Fluids* **26**, 556 (1983).
- [3] D. H. Dubin, J. A. Krommes, C. Oberman, and W. Lee, *The Physics of fluids* **26**, 3524 (1983).
- [4] A. J. Brizard and T. S. Hahm, *Reviews of modern physics* **79**, 421 (2007).
- [5] M. Pueschel, H. Doerk, T. Görler, and F. Jenko, in *37th EPS Conference on Plasma Physics* (European Physical Society, 2010).
- [6] I. Holod and Z. Lin, *Physics of Plasmas* **20** (2013).
- [7] M. J. Pueschel, M. Kammerer, and F. Jenko, *Physics of Plasmas* **15**, 102310 (2008).
- [8] M. Chu, C. Chu, G. Guest, J. Hsu, and T. Ohkawa, *Physical Review Letters* **41**, 247 (1978).
- [9] M. D. Meyers, C.-K. Huang, Y. Zeng, S. Yi, and B. J. Albright, *Journal of Computational Physics* **297**, 565 (2015).

- [10] D. Barnes and L. Chacón, Computer Physics Communications **258**, 107560 (2021).
- [11] H. Ueda, Y. Omura, H. Matsumoto, and T. Okuzawa, [Computer physics communications](#) **79**, 249 (1994).
- [12] X. Jianyuan and Q. Hong, Plasma Science and Technology **23**, 055102 (2021).
- [13] J. Xiao, J. Chen, J. Zheng, H. An, S. Huang, C. Yang, F. Li, Z. Zhang, Y. Huang, W. Han, *et al.*, in *Proceedings of the International Conference for High Performance Computing, Networking, Storage and Analysis* (2021) pp. 1–13.
- [14] A. M. Dimits, G. Bateman, M. Beer, B. Cohen, W. Dorland, G. Hammett, C. Kim, J. Kinsey, M. Kotschenreuther, A. Kritz, *et al.*, [Physics of Plasmas](#) **7**, 969 (2000).
- [15] Z. Liu, Y. Liu, J. Xiao, T. Xia, Y. Li, X. Xu, M. Wu, G. Li, M. Wu, T. Zhang, *et al.*, Nuclear Fusion **62**, 086029 (2022).
- [16] G. Rewoldt, Z. Lin, and Y. Idomura, Computer Physics Communications **177**, 775 (2007).
- [17] X. Garbet, Y. Idomura, L. Villard, and T. Watanabe, Nuclear Fusion **50**, 043002 (2010).
- [18] Y. M. Jeon, Journal of the Korean Physical Society **67**, 843 (2015).